

Dalton Transactions

Inert Cationic Iridium(III) Complexes with Phenanthroline-based Ligands: Application in Antimicrobial Inactivation of Multidrug-Resistant Bacterial Strains

Journal:	*Dalton Transactions*
Manuscript ID	DT-ART-03-2022-000752
Article Type:	Paper
Date Submitted by the Author:	09-Mar-2022

Complete List of Authors:	Busto, Natalia; University of Burgos Faculty of Sciences, Deparment of Chemistry Vigueras, Gloria; Universidad de Murcia, Departmento de Quimica Inorganica Cutillas, Natalia; Universidad de Murcia, Inorganic Chemistry Garcia, Begona; Universidad de Burgos Facultad de Ciencias, Chemistry Department Ruiz, Jose; Universidad de Murcia, Departmento de Quimica Inorganica

Note: The following files were submitted by the author for peer review, but cannot be converted to PDF. You must view these files (e.g. movies) online.
SI JRUIZ.docx

SCHOLARONE™
Manuscripts

ARTICLE

Inert Cationic Iridium(III) Complexes with Phenanthroline-based Ligands: Application in Antimicrobial Inactivation of Multidrug-Resistant Bacterial Strains

Received 00th January 20xx,
Accepted 00th January 20xx

DOI: 10.1039/x0xx00000x

Natalia Busto, †*[a,b] Gloria Vigueras, †[c] Natalia Cutillas,[c] Begoña García*[a] and José Ruiz*[c]

The antimicrobial activity of a new series of heteroleptic iridium(III) complexes of the type $[Ir(C^N)_2(N^N)][PF_6]$ (C^N = deprotonated 2-phenylbenzimidazole-κ*N*, κ*C*; N^N = phen (**Ir1**), dpq (**Ir2**), dppz (**Ir3**), dppn (**Ir4**), and dppz-idzo (**Ir5**)) was studied towards two Gram positive (vancomycin-resistant *Enterococcus faecium* and a methicillin-resistant *Staphylococcus aureus*) and two Gram negative (*Acinetobacter baumanii* and *Pseudomonas aeruginosa*) multidrug-resistant bacterial strains of clinical interest. Although the complexes were inactive towards Gram negative bacteria, their effectivity against Gram positive strains was remarkable, especially for **Ir1** and **Ir2**, the most bactericidal complexes that were even more active (10 times) than the fluoroquinolone antibiotic norfloxacin and displayed no toxicity in human kidney cells (HEK293). Mechanistic studies revealed that the cell wall and membrane of MRSA *S. aureus* remained intact by treatment with these compounds and that DNA was not their main target. Important to note that the complexes were able to induce ROS generation, being this feature key for their antimicrobial activity.

Introduction

Nowadays, antibiotic-resistant infections have become an important cause of morbidity and mortality worldwide. According to the World Health Organization (WHO), each year more than 2.8 million drug-resistant infections happen, resulting in more than 35,000 deaths in the United States. In Europe, antibiotic resistance is responsible for an estimated 33,000 deaths annually.[1] Multidrug-resistant bacteria *Enterococcus faecium*, *Staphylococcus aureus*, *Klebsiella pneumoniae*, *Acinetobacter baumanni*, *Pseudomonas aeruginosa*, and *Enterobacter* species have been identified as the pathogens of most current concern.[2] Particularly, methicillin-resistant *S. aureus* (MRSA), vancomycin-resistant *Enterococcus* (VRE) and fluoroquinolone-resistant *P. aeruginosa* exhibit a quickly rising incidence of infection, with high mortality.[3] Given this serious threat, the discovery of new antibiotics is essential to save modern medicine.

In contrast to traditional organic antimicrobial drugs, which possess a mono or two-dimensional structure, metal complexes are promising in this regard as they provide alternative stereochemical and electronic properties with a tremendous variety of three-dimensional structural scaffolds available through coordination chemistry.[4] These 3D fragments are an ideal starting point for the development of new antibiotics and offer a ready "escape from flatland".[5] In the last years, transition metal complexes have been widely tested as antimicrobial agents.[6–10] These complexes have access to different modes of action such as redox activation, DNA damage, release or exchange of ligands, reactive oxygen species (ROS) generation, etc.[11]

Recent studies on Ir(III) complexes demonstrated that they also exhibit antibacterial properties.[12] Most of the antibacterial agents based on iridium are 'half-sandwich' type complexes.[9,13–18] However, obtaining kinetically inert cyclometalated Ir(III) complexes with antimicrobial properties is less developed.[19–23] In these compounds, the delocalization of the π-electrons over the rings of the chelate ligands was proposed to increase their lipophilicity and promote their penetration into bacterial cell membranes, thereby resulting in bacterial growth inhibition.[24] Previous studies on the antimicrobial properties of metal complexes with ligands based on heteroaromatic derivatives of phenanthrene, such as 1,10-phenanthroline (phen), indicated that inclusion of metal-chelating N,N'-atoms in the phenanthrene ring usually increased the antibacterial activity.[24–26] In addition, the antibacterial activity of phen can be significantly modulated by modifying its structure.[27] Therefore, the development of metal compounds with phen-based ligands provides an opportunity to expand such structural diversity and

[a] *Departamento de Química, Facultad de Ciencias, Universidad de Burgos, Plaza Misael Bañuelos s/n, E-09001, Burgos, Spain, E-mail: nbusto@ubu.es; begar@ubu.es.*
[b] *Departamento de Ciencias de la Salud. Facultad de Ciencias de la Salud. Universidad de Burgos, Hospital Militar, Paseo de los Comendadores, s/n, 09001 Burgos, Spain. E-mail: nbusto@ubu.es*
[c] *Departamento de Química Inorgánica, Universidad de Murcia, and Biomedical Research Institute of Murcia (IMIB-Arrixaca), E-30071 Murcia, Spain, Email: jruiz@um.es.*
† N. B and G. V. contributed equally.
Electronic Supplementary Information (ESI) available: [details of general procedure for the synthesis of Ir(III) complexes, figures for the characterization and stability of the new compounds (NMR, MS), additional figures and tables for their photophysical properties, and figures for cell wall permeabilization and lysis assays]. See DOI: 10.1039/x0xx00000x

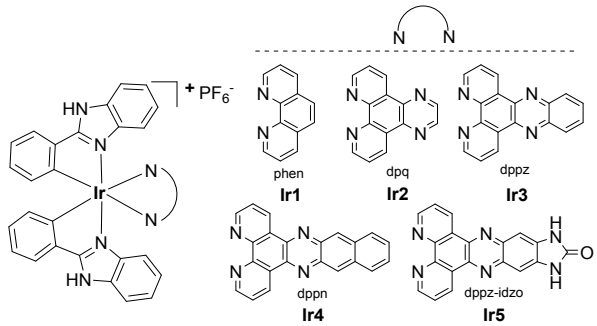
offers the possibility to target different biochemical pathways in bacteria.

Here we have synthetized a series of heteroleptic iridium(III) complexes of the type $[Ir(C^N)_2(N^N)][PF_6]$ (Scheme 1), in which the cyclometalating ligand 2-phenyl-1H-benzo[d]imidazole remains as the C^N backbone and the phenanthroline-based N^N ligand is varied {N^N = phen (**Ir1**), dpq (**Ir2**), dppz (**Ir3**), dppn (**Ir4**), and dppz-idzo (**Ir5**); dpq= dipyrido[3,2-d:2',3'-f]quinoxaline; dppz= dipyrido[3,2-a:2',3'-c]phenazine; dppn= benzo[i]dipyrido[3,2-a:2',3'-c]phenazine; dppz-idzo= dipyrido[3,2-a:2',3'-c]phenazine-10,11-imidazolone}. **Ir3** has been shown prevviously[28] to exhibit interesting photoactivity towards HeLa cancer cells. Herein **Ir3** and the new complexes were investigated as antimicrobial agents against two Gram negative (*A. baumanii* and *P. aeruginosa*) and two Gram positive (*E. faecium* and *S. aureus*) bacteria of clinical interest. Their toxicity against healthy human embryonic kidney cells was also evaluated.

Results and Discussion

Synthesis and characterization

As metal complexes with phenanthroline-based ligands have strong antibacterial potential, we aimed to develop novel iridium complexes based on this type of N^N ligands. For this purpose, a series of five substitutionally inert Ir(III) complexes of the type $[Ir(C^N)_2(N^N)][PF_6]$ (Scheme 1) were synthesized and characterized. Complexes **Ir1–Ir5** were obtained in high yields (55–84%) by the reaction of the cyclometalated dinuclear Ir(III) complex with the different N^N ligands in a 1:2 molar ratio in a similar manner to previously reported methods.[28,29] **Ir1–Ir5** were characterized by ^1H and ^{13}C NMR spectroscopy (Figures S1-S5) and positive-ion ESI-HRMS (Figures S6-S9). All compounds were shown to be at least 95% pure by both elemental analysis and reverse-phase RP-HPLC in DMSO (Figures S6-S9). The positive ion ESI mass spectra displayed the $[M-PF_6]^+$ signals with the expected isotopic distribution pattern. The stability of the complexes in solution was studied by ^1H NMR spectroscopy and UV/Vis. No changes in the spectra were detected after 24 h at room temperature in DMSO and water solutions (Figures S10-S11).



Scheme 1. Structures of the Ir(III) complexes investigated in this work.

Photophysical properties

The UV/Vis absorption spectra of complexes (Figure 1 and S12) were recorded in water (1% DMSO, 10 µM) and acetonitrile (10 µM). All complexes exhibit characteristic absorptions of the bis-cyclometalated iridium complexes (Table S2).[30,31] Between 230 and 330 nm, it can be observed intense bands (molar extinction coefficients of the order of 10^3 $M^{-1}cm^{-1}$) assigned to the permitted transitions centered on the ligands ($^1\pi$-π^*). On the other hand, the broad bands of lower energy between 330 and 440 nm and the rest of weak absorptions between 440-520 nm could be assigned to ^{1}MLCT,^{3}MLCT ($d\pi$ (Ir) → π^*) and ^{1,3}LLCT transitions.[31,32] Upon excitation at the absorption wavelength maxima, all complexes showed yellow to orange emissions in acetonitrile (Figure S13), while in water, only **Ir1**, **Ir2** and **Ir3** exhibited orange phosphorescent emissions (Figure 1), being **Ir3** containing dppz, the complex with the weakest emission. This characteristic is common for other Ir(III) compounds with the dppz ligand.[28,29,33] In addition, the decrease of the emission quantum yields and the quenching of the luminescence of **Ir4** and **Ir5** by the water could also be explained by the increase of the non-radiative process due to the interaction of the solvent with the two uncoordinated basic nitrogens of the ligands.[34,35]

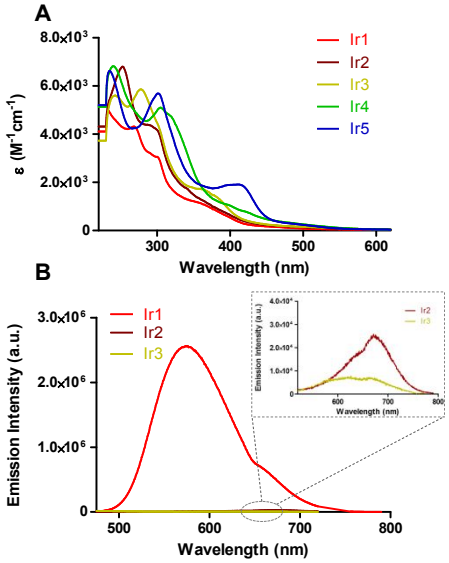


Figure 1. A) UV/Vis spectra of new complexes in water and B) Emission spectra of **Ir1**-**Ir3** in aerated water solution at 10 µM. λexc =370 nm.

The photophysical properties in water are further summarized in Table 1. As observed, their luminescence lifetimes in water (1% DMSO) are consistent with the triplet nature of the emission state.[31]

Table 1. Excitation (λ_{exc}), emission (λ_{em}) wavelengths, emission lifetimes (τ_{em}), and quantum yields (Φ_{em}) of **Ir1**, **Ir2** and **Ir3** in deaerated water (1% DMSO).

Compound	λ_{exc}, nm[a]	λ_{em}, nm	τ_{em}, ns[b]	Φ_{em},% [b]
Ir1	370	573	54 (40%) 335 (60%)	5.1
Ir2	375	667	390 (100%)	1.0
Ir3	385	621	46 (4%) 308 (96%)	<1

[a] λ_{exc} maxima. [b]20 min under argon.

This journal is © The Royal Society of Chemistry 20xx

Antimicrobial activity

The ability of these iridium(III) complexes to inhibit the growth of two Gram positive (VR *E. faecium* and MRSA *S. aureus*) and two Gram negative (*A. baumanii* 17978 and *P. aeruginosa* PAO1) strains were studied using the broth microdilution method. Their activities were expressed as minimal inhibitory concentration (MIC) values, that is, the lowest concentration of the compound that prevents bacterial growth. As observed in Table 2, all complexes were active against the studied Gram positive bacteria, whereas they were completely inactive (with MICs over 100 µM) against the Gram negative bacteria. With impressive values of MIC, complexes Ir1 and Ir2 were even more effective than the broad-spectrum fluoroquinolone antibiotic norfloxacin in both VR *E. faecium* and MRSA *S.aureus* strains, showing Ir1 an inhibitory capacity 10 times greater than this reference antibiotic in MRSA *S.aureus*. On the other hand, Ir4 exhibited a remarkable activity only against VR *E. faecium* and Ir3 displayed the lowest antimicrobial activity of the family.

Table 2. MIC values (µM) of the Ir complexes. Norfloxacin it is included as positive control.

	MIC, µM			
	Gram Positive		Gram Negative	
	E. faecium	*S. aureus*	*A. baumanii*	*P. aeruginosa*
Ir1	3	0.6	> 100	> 100
Ir2	5	2.5	100	> 100
Ir3	40	40	> 100	> 100
Ir4	4	20	> 100	> 100
Ir5	20	10	100	> 100
Norfloxacin	6	6	20	3

In order to determine if the complexes can be classified as bacteriostatic or bactericidal agents, the minimal bactericidal concentrations (MBC) were determined (Table 3). According to the ratio MBC/MIC, we can defined the antimicrobial agents as bactericidal complexes if MBC/MIC ≤ 4 or bacteriostatic agents if the ratio MBC/MIC > 4.[36] **Therefore, complexes Ir1, Ir2, Ir3 and Ir5, were clearly bactericidal complexes whereas Ir4 displayed a bacteriostatic effect.**

Table 3. MBC values of the Ir complexes.

	MBC, µM			
	Gram Positive		Gram Negative	
	E. faecium	*S. aureus*	*A. baumanii*	*P. aeruginosa*
Ir1	5	2	> 100	> 100
Ir2	5	2.5	> 100	> 100
Ir3	> 100	40	> 100	> 100
Ir4	>100	>100	> 100	> 100
Ir5	40	40	> 100	> 100

Toxicity in human cells

To further evaluate the potential of these Ir(III) polypyridyl complexes as antimicrobial agents, studying their cytotoxicity towards human cells is mandatory. Therefore, the antiproliferative activity of these compounds was evaluated using standard MTT assay in human embryonic kidney cells, HEK293 (Figure 2). All complexes except Ir3, could be considered as not cytotoxic in human cells. Ir3 displayed antiproliferative activity (IC_{50} = 27.0 µM ± 1.5) being more toxic to human cells than to bacteria.

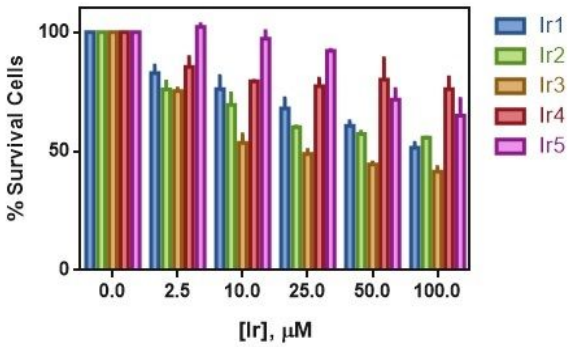


Figure 2. Dose-response plots of the Ir(III) complexes in HEK293 cells after 24 h of treatment.

Gram negative bacteria resistance

The low permeability barrier of Gram negative bacteria renders the discovery of new antibiotics against these bacteria a challenging issue.[13,37,38] **As these Ir(III) compounds exerted no antimicrobial activity against Gram negative bacteria (Table 2), we studied if the extra outer membrane of these bacteria was hindering the uptake of the complexes. It is well-known that EDTA induces outer membrane permeabilization,**[39] **so we tested if, upon permeabilization of the membrane with EDTA, the complexes displayed some activity against *P. aeruginosa* PAO1. MIC determination was performed in the presence of 0.5 mM of EDTA, and then, MBC was also evaluated (Table 4). Although the complexes were completely inactive in the absence of EDTA, in its presence, all the compounds displayed some activity. Therefore, EDTA was able to sensitize *P. aeruginosa*, increasing the sensitizing effect in the complexes with the lower degree of the π conjugation of the phen-based ligand.**

Table 4. MIC and MBC values of the Ir complexes against *P. aeruginosa* in the presence of 0.5 mM of EDTA. The shown MIC and MBC values in the absence of EDTA were included again for clarity.

	MIC (EDTA), µM	MBC (EDTA), µM	MIC, µM	MBC, µM
Ir1	12.5	100	> 100	> 100
Ir2	25	> 100	> 100	> 100
Ir3	50	> 100	> 100	> 100

Ir4	75	> 100	> 100	> 100
Ir5	75	> 100	> 100	> 100

The outer membrane permeabilization by EDTA and its potential implication in the cellular uptake of the Ir(III) complexes was investigated by ICP-MS experiments. Cellular accumulation with and without EDTA treatment revealed that EDTA increased the uptake of the Ir(III) complexes (Figure 3), further supporting the results shown in Table 4.

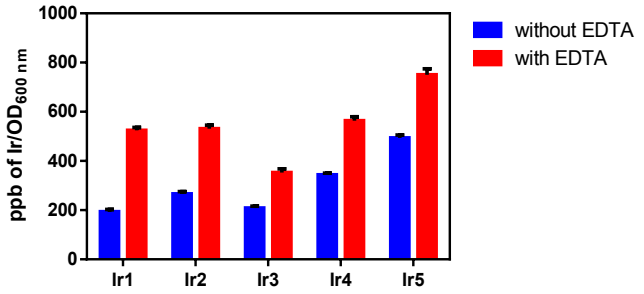


Figure 3. Ir accumulation in *P. aeruginosa* treated with and without 0.5 mM of EDTA and 1 µM of the Ir(III) complexes.

Mechanism of action in gram positive strains

Kinetics of growth inhibition. The kinetics of growth inhibition by the Ir(III) complexes were studied in MRSA *S. aureus* and VR *E. faecium* for 24 and 12 h, respectively at two concentrations: below the determined MICs (0.5 × MIC) and the MICs values. As observed in the MRSA *S. aureus* growth curves (Figure 4), **Ir4** lead to a modest delay in reaching the logarithmic growth phase in comparison to the control, reinforcing its bacteriostatic effect. **Ir5** induced a most evident delay (≈ 14 h) at MIC concentration which confirmed its bactericidal effect. On the other hand, **Ir1** and **Ir3** completely inhibited MRSA *S. aureus* growth at their MIC concentration as well as **Ir2,** which inhibited bacterial growth even at concentrations below the MIC.

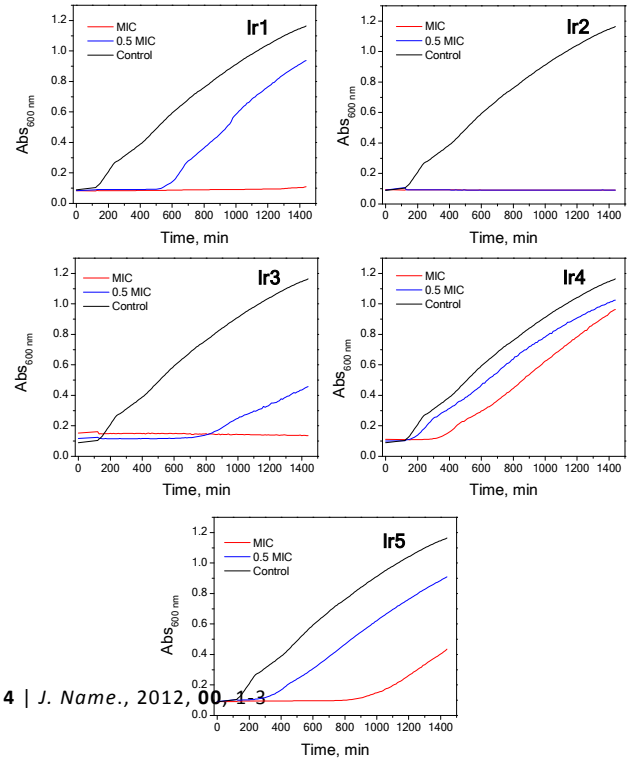


Figure 4. Growth curves of MRSA *S. aureus* incubated with 0.5% DMSO (Control) and at concentrations 0.5 MIC and MIC of the Ir(III) complexes.

Regarding to VR *E. faecium* growth curves (Figure 5)**, all complexes except Ir4 exerted a bactericidal effect since the bacterial growth was completely inhibited even at the lowest concentration tested. By contrast, Ir4 showed a slight delay (less than 6 h) to reach the logarithmic growth phase, confirming its bacteriostatic behavior.**

Cell wall permeabilization and lysis. The cell wall and cell membrane of bacteria are two major targets in antibiotic development. Therefore, we investigated if the new Ir complexes were able to kill bacteria by cell leakage. Cell permeabilization was studied by measuring propidium iodide (PI) fluorescence. This dye cannot be internalized if the cell membrane is not damaged, but once inside the cell, PI intercalates into DNA base-pairs enhancing its fluorescence. Thus, MRSA *S. aureus* was incubated for 2 h with the Ir(III) complexes at both the MBC and 4× MBC. Then, PI was added and the fluorescence was monitored for an hour. No changes were observed (Figure S14A), so in principle, no leakage occurred.

To better support these results, the OD_{600nm} was monitored for 2 h with the iridium complexes and treatment did not lead to any decrease in the OD_{600nm} (data not shown). Moreover, upon the 2 h of treatment, no leakage of the intracellular contents was detected, since the OD_{260nm} stayed unchanged (Figure S14B). Thus, cell membrane remained intact upon treatment

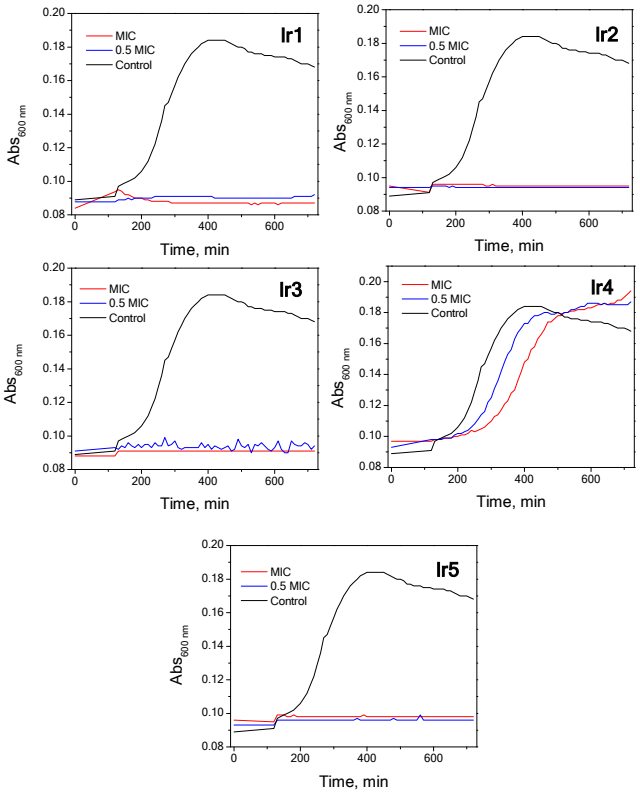


Figure 5. Growth curves VR *E. faecium* incubated with 0.5% DMSO (Control) and at concentrations 0.5 MIC and MIC of the Ir(III) complexes.

with 4×MBC and the mechanism of action of these complexes seems to be not related to cell wall permeabilization in contrast

This journal is © The Royal Society of Chemistry 20xx

with the reported mechanism of action of other antimicrobial ruthenium(II)[40] and Ir(III) agents.[23]

Oxidative stress. Bacteria death can occur due to oxidative stress. Indeed, it has been described how bactericidal agents are able to produce reactive oxygen species (ROS) as products of the tricarboxylic acid cycle, due to NADH depletion, hyperactivation of electron transport that increases superoxide levels, destabilization of iron-sulfur clusters, and an increase of the Fenton reaction.[41] In the last years, ROS generation has been reported as a mechanism of action of some antibacterial Ir(III) complexes.[23,42,43] In order to shed some light on the mechanism of action of these complexes towards Gram positive strains, we evaluated their activity in the presence of N-acetyl-cysteine (NAC), a ROS inhibitor. As observed in Table 5, NAC treatment slightly increased MIC values of **Ir2** and **Ir4**, whereas the rise was moderate for **Ir1** and **Ir5** and almost no effect of NAC treatment was detected for **Ir3**. Although these complexes may induce ROS generation, this mechanism is not straightforwardly supported by these results with NAC treatment. Thus, ROS generation was also studied by flow cytometry in MRSA *S. aureus* treated with 2',7'-dichlorofluorescein diacetate (DCF-DA). As observed in Figure 6, all complexes were able to increase ROS levels at both concentrations (0.5 × MIC and MIC values). Therefore, ROS generation seems to be key for the antimicrobial activity of the new complexes.

Table 5. MIC values in MRSA *S. aureus* of the iridium complexes in bacteria treated with 1 mM of NAC.

	MIC (NAC), μM	MIC(NAC)/MIC ratio
Ir1	2.5	4.2
Ir2	5	2
Ir3	40	1
Ir4	40	2
Ir5	40	4

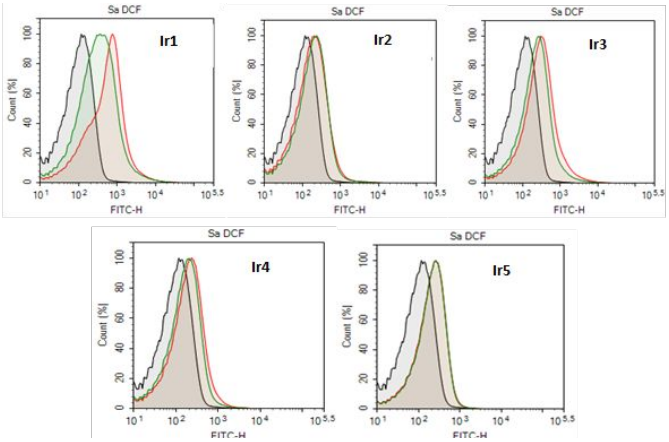


Figure 6. ROS production detection using H_2DCFDA after 2 h incubation of MRSA *S. aureus* with the Ir complexes by flow cytometry. Vehicle (grey profile), 0.5 MIC (green profile) and MIC (red profile).

Interaction with plasmid DNA. Targeting DNA replication is one of the main strategies in the design of novel antibiotics able to circumvent resistance.[44] Quinolones, for instance, are well-known bactericidal antibiotics whose mechanism of action is based on inhibiting DNA gyrase or Topoisomerase IV by binding to the complex formed between these enzymes and DNA.[45] Therefore, DNA binding of the Ir(III) complexes was investigated by a gel mobility assay. The plasmid pUC18 (extracted from *E. coli* DH5α) was incubated overnight at 37°C with different concentrations of the Ir(III) complexes. Since no differences in the migration pattern of the plasmid were detected, covalent binding and intercalation processes were discarded (Figure 7).

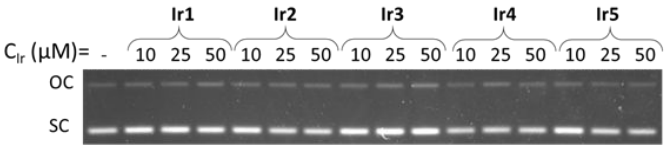


Figure 7. Electrophoresis of pUC18 alone (1st lane) and in the presence of different concentrations of the Ir(III) complexes.

On the other hand, it has been reported that the biological reducing agent glutathione (GSH) can activate the catalytic DNA cleavage activity of some Ru(II) polypyridyl complexes in cell-free media.[46] GSH is not only found in eukaryotic cells, but can also be found in gram negative bacteria. However, except for some streptococcus and enterococcus species, it is not found in gram positive bacteria, where other antioxidants thiols are present. In fact, bacillithiol (BSH) is the main low molecular thiol controlling redox homeostasis in staphylococcus.[47,48] Therefore, we wonder if the synthesized Ir(III) complexes were able to produce DNA cleavage in the presence of GSH as a model of an antioxidant low molecular thiol. As shown in Figure 8, **Ir1** and **Ir2** clearly cleaved DNA in a concentration-dependent manner, increasing the open circular form (OC) and decreasing the supercoiled form (SC). The linear form did not appear indicating that single strands break (SSB) occurred. These cell-free data suggest that a single-strand cleavage of DNA could occur inside the bacteria due to a redox-cycling[46] mediated by the complexes containing phen and dpq ligands and a thiol reductant, which could explain the greater antibacterial capacity of **Ir1** and **Ir2**.

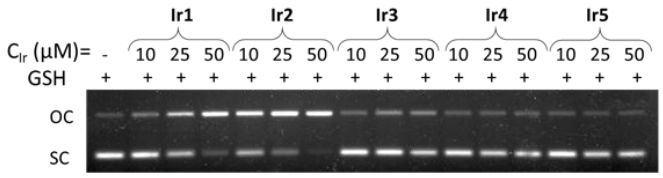


Figure 8. Agarose gel electrophoresis of the DNA cleavage products of pUC18 after 4 h of incubation with 120 μM of GSH and different concentrations of the Ir(III) complexes.

Conclusions

In summary, we report the synthesis, characterisation and antimicrobial activity of a series of cationic inert bis-cyclometalated Ir(III) complexes **Ir1**-**Ir5** (C^N = deprotonated 2-phenylbenzimidazole) and a phenanthroline-based N^N ligand showing different degrees of the π conjugation. Quenching of the luminescence by water was observed for complexes **Ir4** and **Ir5**, whereas **Ir1**, **Ir2**, and **Ir3** exhibited orange phosphorescent emissions in this solvent. Although the investigated iridium complexes were completely inactive against Gram negative bacteria due to the extra outer membrane that hinders their internalization, these compounds turned out to be promising antimicrobial agents against Gram positive bacteria, except **Ir4**, which was a bacteriostatic antimicrobial complex. Remarkably, **Ir1** and **Ir2** were even more effective than the broad-spectrum fluoroquinolone antibiotic norfloxacin in both VR *E. faecium* and MRSA *S. aureus* strains, showing **Ir1** an inhibitory capacity 10 times greater than this reference antibiotic in MRSA *S. aureus*. Mechanistic studies revealed that the cell wall and membrane of MRSA *S. aureus* remained intact by treatment with these compounds. Furthermore, DNA was not the main target of these iridium compounds. Important to note that their activity seems to be related to oxidative stress induction since all of them were able to stimulate ROS generation. Moreover, in the presence of the biological reductant glutathione, the complexes **Ir1** and **Ir2** clearly cleaved DNA in a concentration-dependent manner, which could explain their greater antibacterial capacity.

This study reveals that among this family of iridium compounds, **Ir1** and **Ir2**, with the lowest degree of the π-conjugation of the organic N^N ligand (phen and dpq, respectively), are the most promising candidates as Gram positive bactericidal antibiotics to be further explored.

Experimental

Materials and instrumentation

Starting materials: $IrCl_3 \cdot H_2O$ was used as received (Johnson Matthey). The pro-ligand 2-phenyl-1H-benzo [d]imidazole was obtained from Merk (Madrid, Spain). Deuterated solvents were purchased from Euriso-top. The C, H, and N analyses were performed with a Carlo Erba model EA 1108 microanalyzer. The ^{1}H and ^{13}C spectra were recorded on a Bruker AC 300E, Bruker AV 400, or Bruker AV 600 NMR spectrometer and chemical shifts are cited relative to $SiMe_4$ (^{1}H and ^{13}C, external). ESI mass (positive mode) analyses were carried out on an HPLC/MS TOF 6220. In every case, the isotopic distribution of the heaviest set of peaks matched very closely with that calculated for the formulation of the complex cation. The purity of all biologically evaluated molecules, based on HPLC and elemental analysis, is >95%. Ir(III) complexes were always freshly prepared in DMSO before use.

Synthesis methods and characterization

The cyclometalating pro-ligand 2-phenyl-1H-benzo [d]imidazole is commercial. The quinoxaline and phenazine ligands (dpq, dppz, dppn and dppz-idzo) were synthesized through Schiff-base condensation of 1,10-phenantroline-5,6-dione (phendio) with ethylenediamine, o-phenylenediamine, 2,3-diaminonaphthalene, and 5,6-diaminobenzimidazolone-2 as previously reported.[49,50]

Preparation of monomeric Ir(III) compounds. The method was adapted from the previously described.[51–53] **The experimental details are shown in the Supporting Information.**

Ir1. Bright orange solid. Isolated yield: 55%. ^{1}H-NMR (400 MHz, [D_6]DMSO): δ 14.28 (s, NH, 2H), 8.91 (dd, J = 8.0, 1.2 Hz, 2H), 8.49 (dd, J = 4.9, 1.1 Hz, 2H), 8.35 (s, 2H), 8.10 (dd, J = 8.3, 5.2 Hz, 2H), 8.02 (d, J = 7.7 Hz, 2H), 7.54 (d, J = 8.2 Hz, 2H), 7.09 (m, 4H), 6.88 (t, J = 7.3 Hz, 2H), 6.71 (t, J = 7.3 Hz, 2H), 6.36 (d, J = 7.5 Hz, 2H), 5.28 (d, J = 8.2 Hz, 2H). ^{13}C- NMR (100 MHz, [D_6]DMSO): δ 164.68, 152.06, 150.14, 147.90, 139.64, 139.08, 134.83, 133.64, 133.25, 130.93, 130.85, 128.67, 127.35, 124.98, 123.76, 123.53, 122.59, 113.58, 112.84; ESI-MS (pos. ion mode, DMSO): m/z = 759.1860 [M-PF_6]$^+$. Anal. Calcd. for $C_{38}H_{26}F_6IrN_6P$: C, 50.50; H, 2.90; N, 9.30. Found: C, 50.74; H, 2.91; N, 9.32 (%).

Ir2. Orange solid. Isolated yield: 79%. ^{1}H-NMR (600 MHz, [D_6]DMSO): δ 14.20 (s, NH, 2H), 9.67 (dd, J = 8.3, 1.2 Hz, 2H), 9.31 (s, 2H), 8.60 (dd, J = 4.8, 1.1 Hz, 2H), 8.25 (m, 2H), 8.00 (d, J = 7.6 Hz, 2H), 7.53 (d, J = 8.0 Hz, 2H), 7.08 (m, 4H), 6.89 (dt, J = 7.6, 1.2 Hz, 2H), 6.73 (t, J = 7.6 Hz, 2H), 6.32 (d, J = 7.6 Hz, 2H), 5.45 (d, J = 8.0 Hz, 2H). ^{13}C-NMR (150 MHz, [D_6]DMSO): δ 164.65, 154.38, 150.80, 150.46, 148.38, 140.68, 140.55, 136.26, 135.77, 134.64, 134.14, 131.94, 130.80, 129.61, 125.97, 124.93, 124.56, 123.73, 114.51, 114.26; ESI-MS (pos ion mode, DMSO): m/z = 811.1919 [M-PF_6]$^+$. Anal. Calcd. for $C_{40}H_{26}F_6IrN_8P$: C, 50.26; H, 2.74; N, 11.72. Found: C, 50.45; H, 2.75; N, 11.76 (%).

Ir3. Orangish brown solid. Isolated yield: 83%. Reported.[28]

Ir4. Reddish solid. Isolated yield: 82%. ^{1}H-NMR (600 MHz, [D_6]DMSO): δ 14.14 (s, NH, 2H), 9.44 (d, J = 7.8, 2H), 8.73 (s, 2H), 8.53 (d, J = 4.8, 2H), 8.13 (m, 2H), 8.04 (m, 2H), 8.00 (d, J = 7.2, 2H), 7.57 (d, J = 8.0 Hz, 2H), 7.57 (m, 2H), 7.12 (m, 4H), 6.91 (t, J = 7.5 Hz, 2H), 6.84 (t, J = 8.1 Hz, 2H), 6.35 (d, J = 7.5 Hz, 2H), 5.71 (d, J = 8.4 Hz, 2H). ^{13}C-NMR (150 MHz, [D_6]DMSO): δ 165.71, 154.36, 152.18, 150.82, 141.68, 140.80, 139.07, 136.21, 135.72, 134.69, 134.16, 132.02, 131.64, 129.83, 129.76, 129.19, 129.05, 125.94, 125.11, 124.71, 123.82, 114.76, 114.55; ESI-MS (pos ion mode, DMSO): m/z = 911.2249 [M-PF_6]$^+$. Anal. Calcd. for $C_{48}H_{30}F_6IrN_8P$: C, 54.59; H, 2.86; N, 10.61. Found: C, 54.86; H, 2.88; N, 10.54 (%).

Ir5. Red solid. Isolated yield: 84%. ^{1}H-NMR (400 MHz, [D_6]DMSO): δ 14.06 (s, NH, 2H), 11.67 (s, 2H), 9.56 (d, J = 8.0 Hz, 2H), 8.54 (dd, J = 5.2, 1.2 Hz, 2H), 8.15 (m, 2H), 7.98 (d, J = 7.4, 2H), 7.55 (m, 4H), 7.11 (m, 4H), 6.92 (t, J = 7.6 Hz, 2H), 6.77 (t, J = 7.6 Hz, 2H), 6.35 (d, J = 7.6 Hz, 2H), 5.56 (d, J = 8.4 Hz, 2H). ^{13}C-NMR (100 MHz, [D_6]DMSO): δ 164.69, 156.41, 152.62, 150.05, 149.69, 140.52, 139.75, 137.93, 136.68, 134.76, 133.67, 133.18, 130.97, 130.41, 128.37, 124.88, 123.99, 123.62, 122.73, 113.55, 113.38, 103.70; ESI-MS (pos ion mode, DMSO): m/z = 917.2110 [M-PF_6]$^+$. Anal. Calcd. for $C_{48}H_{28}F_6IrN_{10}OP$: C, 50.90; H, 2.66; N, 13.19. Found: C, 50.98; H, 2.68; N, 13.15 (%).

RP-HPLC purity and stability analyses

This journal is © The Royal Society of Chemistry 20xx

The experimental details are described in the Supporting Information.

Photophysical characterization

UV/Vis spectroscopy was carried out on a PerkinElmer Lambda 750 S spectrometer with operating software. Solutions of all complexes were prepared in acetonitrile and water (1% DMSO) at 10 μM. Emission spectra were obtained with a Horiba Jobin Yvon Fluorolog 3–22 modular spectrofluorometer with a 450 W xenon lamp. Measurements were performed in a right angle configuration using 10 mm quartz fluorescence cells for solutions at 298 K. Emission lifetimes (τ) were measured using an IBH FluoroHub TCSPC controller and a NanoLED (372 nm) pulse diode excitation source (τ < 10μs); the estimated uncertainty is ±10% or better. Emission quantum yields (Φ) were measured using a Hamamatsu C11347 Absolute PL Quantum Yield Spectrometer; the estimated uncertainty is ±5% or better. Solutions of all complexes were prepared in acetonitrile and water (1% DMSO) at 10 μM. For lifetimes and quantum yields measurements the samples were previously degassed by bubbling argon for 20 min.

Bacterial strains

E. faecium CECT 5253 (vancomycin resistant, Gram positive bacteria) was maintained in Tryptic Soy (TS) broth or agar while *S. aureus* CECT 5190 (methicillin resistant, Gram positive bacteria), *A. baumannii* ATCC 17978 (Gram negative bacteria) and *P. aeruginosa* PAO1 (Gram negative bacteria) were maintained in Mueller-Hinton (MH) broth or agar at 37 ºC.

Antibacterial activity: MIC and MBC determination

The antibacterial activity was evaluated by the broth microdilution plate method according to CLSI criteria against ESKAPE (*Enterococcus faecium*, *Staphylococcus aureus*, *Klebsiella pneumoniae*, *Acinetobacter baumannii*, *Pseudomonas aeruginosa*, and *Enterobacter cloacae*) pathogens.[54] Briefly, serial dilutions of the compounds were prepared in MHB (1:2 dilutions) in 96-well plates. Norfloxacin was used as the positive control. An initial inoculum of every strain was prepared at 0.5 McFarland in water and immediately diluted in MHB (1:20). Then, plates were inoculated with 5 μL of the bacterial dilution leading to a concentration of 5×10^5 CFU/mL and incubated at 37 ºC for 18-20 h. The uninoculated broth was used as the sterility control and the inoculated broth without drugs was used as the growth control.

In the case of MIC determination upon EDTA (Disodium ethylenediaminetetraacetate) permeabilization, 0.5 mM of EDTA was added to each well, and control with only EDTA was also included.

For MIC evaluation in the presence of the ROS inhibitor N-acetyl-L-cysteine (NAC), MIC was determined as explained above but in the presence of 1 mM of NAC per well. As with EDTA, the effect of this concentration of NAC on bacterial growth was tested.

The minimal bactericidal concentrations (MBC) were determined by plating in MHA 10 μL of the sample solutions from each well with no visible growth in MIC determination plates. The agar plates were incubated for another 20 h and at 37°C. The concentration at which no colonies had been formed correspond to the MBC values.

Kinetic growth curves

Overnight cultures of the two pathogenic Gram positive strains (VR *E. faecium* and MRSA *S. aureus*) were then diluted to 0.5 McFarland in fresh MHB. A bacterial suspension of 1.0×10^5 CFU/mL was prepared in 24 well-plates and treated with the Ir(III) complexes at concentrations equal to 0.5 × MIC and the MIC value. Wells with bacteria treated with the vehicle (0.5 % DMSO) and not treated were included as vehicle and negative controls. The growth rate was monitored by recording the OD600 every 10 min for 24 h in a microplate reader (Cytation 5 Cell Imaging Multi-Mode Reader (Biotek Instruments, USA)). Each condition was tested in quadruplicate.

Uptake by ICP-MS

Bacterial inocula in the log phase were adjusted to 0.5 McFarland and then diluted 1:100 in conical tubes with 5 mL of fresh MHB, with and without 0.5 mM of EDTA and 1 μM of the Ir(III) complexes. Samples were incubated overnight at 37°C and 120 rpm. Then, bacteria were centrifuged at 8000 rpm for 10 min. The pellet was washed twice with phosphate buffer saline (PBS) and finally, resuspended in 1 mL of PBS. 20 μL were used to record the OD_{600} in a microplate reader (Cytation 5 Cell Imaging Multi-Mode Read-er (Biotek Instruments, USA)). The samples were digested with 65% HNO_3 at room temperature for 24 h. Lastly, solutions were analyzed in an 8900 ICP-MS (Agilent Technologies). Data are reported as the mean of two independent experiments with two replicates for each condition assayed.

Cell wall permeabilization and lysis assay

Overnight cultures of MRSA *S. aureus* in MHB were centrifuged at 8000 rpm for 10 min. The supernatant was removed and the pellet resuspended and diluted in fresh MHB to give 0.5 McFarland. 20 μL of the bacterial suspension were added to an optical black-side 96-wells plate containing the iridium complexes at concentrations equal to their MBC and 4 × MBC values when possible, being 200 μM the highest concentration tested. A negative control (bacteria without treatment) and vehicle control (0.8% DMSO) were included. After 2 h of incubation at 37°C, 10 μL of propidium iodide 10 mg/mL were added to each well. The fluorescence at 617 nm (λ_{exc} = 535 nm) was monitored every 10 min for 1 h. Positive control of bacteria treated for 30 min with ethanol 70% was also included. Each condition was tested in triplicate.

Cellular leakage and lysis were also assayed by monitoring the OD_{600} at the beginning and for 2 h of incubation with the Ir complexes. The lysis assay[55] was performed by recording the OD_{260nm} of filtrated (0.2 μm) samples at t=0 and t=2 h in a black side quartz 96-wells plate. The blank (containing only medium)

was subtracted. Two samples of each tested condition were included and the experiment was conducted twice.

ROS generation by flow cytometry

Overnight cultures of MRSA *S. aureus* in MHB were centrifuged at 8000 rpm for 10 min. The pellet was resuspended and a bacterial dilution adjusted to 0.5 McFarland was prepared. A final bacterial concentration of 1.5 × 10^6 cfu/mL in fresh MHB containing 25 µM of H2DCFDA (2'-7'-dichlorofluorescein diacetate) was treated with the iridium complexes at concentrations equal to 0.5×MIC and MIC values for 2 h. Then, bacteria were centrifuged at 8000 rpm for 10 min. The pellets were washed twice with PBS. Finally, the pellets were resuspended in 150 µL of PBS and analyzed using the NovoCyte Flow cytometer (ACEA Biosciences, Inc., USA).

Agarose gel electrophoresis

Overnight cultures of the strain DH5α of Escherichia coli were isolated with the Quiagen DNA purification kit. 20 µM (in base pairs) of plasmid DNA (pUC18) was incubated with different concentrations of the synthesized iridium complexes overnight at 37°C for the DNA mobility assay. For the DNA cleavage assay, 20 µM of pUC18 was incubated for 4 h at 37°C with 120 µM of GSH and the same concentrations of the Ir complexes employed in the mobility assay. Afterward, 2 µL of loading buffer were added to 10 µL of the incubated samples and loaded onto a 1% agarose gel. Electrophoresis was run at 5.5 V/cm for 2 h. The agarose gel was immersed in a solution of ethidium bromide 1 µg/mL in TAE 1× for 30 minutes. Then, the gel was destained with TAE 1× for 10 minutes and visualized with a Gel Doc XR+ Imaging System (Bio-Rad).

Author Contributions

N. B. and G. V. contributed equally to this work. The manuscript was written through contributions of all authors. All authors have given approval to the final version of the manuscript.

Conflicts of interest

There are no conflicts to declare.

Acknowledgements

This work was supported by the Spanish Ministerio de Ciencia e Innovación (MCI/AEI) and FEDER funds (Projects RTI2018-096891-B-I00, RTI2018-102040-B-100 and MultiMetDrugs network RED2018-102471-T), Fundación Séneca-Región de Murcia (project 20857/PI/18), Consejería de Educación-Junta de Castilla y León-FEDER (BU042U16-BU305P18) and "la Caixa" Banking Foundation (LCF/PR/PR12/11070003). G.V. thanks the University of Murcia for a grant (R-1034/2016). We are indebted to M. Mansilla and T. Gil-Antón (Universidad de Burgos) for technical support.

Notes and references

1 World Health Organization, *2019 antibacterial agents in clinical development: an analysis of the antibacterial clinical development pipeline*, World Health Organization, Geneva, 2019.
2 F. Li, J. G. Collins and F. R. Keene, Ruthenium complexes as antimicrobial agents, *Chem. Soc. Rev.*, 2015, **44**, 2529–2542.
3 H. W. Boucher, G. H. Talbot, J. S. Bradley, J. E. Edwards, D. Gilbert, L. B. Rice, M. Scheld, B. Spellberg and J. Bartlett, Bad Bugs, No Drugs: No ESKAPE! An Update from the Infectious Diseases Society of America, *Clinical Infectious Diseases*, 2009, **48**, 1–12.
4 C. N. Morrison, K. E. Prosser, R. W. Stokes, A. Cordes, N. Metzler-Nolte and S. M. Cohen, Expanding medicinal chemistry into 3D space: metallofragments as 3D scaffolds for fragment-based drug discovery, *Chem. Sci.*, 2020, **11**, 1216–1225.
5 F. Lovering, J. Bikker and C. Humblet, Escape from Flatland: Increasing Saturation as an Approach to Improving Clinical Success, *J. Med. Chem.*, 2009, **52**, 6752–6756.
6 M. Patra, G. Gasser and N. Metzler-Nolte, Small organometallic compounds as antibacterial agents, *Dalton Trans.*, 2012, **41**, 6350–6358.
7 M. Patra, M. Wenzel, P. Prochnow, V. Pierroz, G. Gasser, J. E. Bandow and N. Metzler-Nolte, An organometallic structure-activity relationship study reveals the essential role of a $Re(CO)_3$ moiety in the activity against gram-positive pathogens including MRSA, *Chem. Sci.*, 2015, **6**, 214–224.
8 D. K. Weber, M.-A. Sani, M. T. Downton, F. Separovic, F. R. Keene and J. G. Collins, Membrane Insertion of a Dinuclear Polypyridylruthenium(II) Complex Revealed by Solid-State NMR and Molecular Dynamics Simulation: Implications for Selective Antibacterial Activity, *J. Am. Chem. Soc.*, 2016, **138**, 15267–15277.
9 P. Chellan, V. M. Avery, S. Duffy, J. A. Triccas, G. Nagalingam, C. Tam, L. W. Cheng, J. Liu, K. M. Land, G. J. Clarkson, I. Romero-Canelón and P. J. Sadler, Organometallic Conjugates of the Drug Sulfadoxine for Combatting Antimicrobial Resistance, *Chemistry – A European Journal*, 2018, **24**, 10078–10090.
10 K. L. Smitten, S. D. Fairbanks, C. C. Robertson, J. Bernardino de la Serna, S. J. Foster and J. A. Thomas, Ruthenium based antimicrobial theranostics – using nanoscopy to identify therapeutic targets and resistance mechanisms in Staphylococcus aureus, *Chem. Sci.*, 2020, **11**, 70–79.
11 A. Frei, J. Zuegg, A. G. Elliott, M. Baker, S. Braese, C. Brown, F. Chen, C. G. Dowson, G. Dujardin, N. Jung, A. P. King, A. M. Mansour, M. Massi, J. Moat, H. A. Mohamed, A. K. Renfrew, P. J. Rutledge, P. J. Sadler, M. H. Todd, C. E. Willans, J. J. Wilson, M. A. Cooper and M. A. T. Blaskovich, Metal complexes as a promising source for new antibiotics, *Chem. Sci.*, 2020, **11**, 2627–2639.
12 A. Zamora, G. Vigueras, V. Rodríguez, M. D. Santana and J. Ruiz, Cyclometalated iridium(III) luminescent complexes in therapy and phototherapy, *Coordination Chemistry Reviews*, 2018, **360**, 34–76.
13 F. Chen, J. Moat, D. McFeely, G. Clarkson, I. J. Hands-Portman, J. P. Furner-Pardoe, F. Harrison, C. G. Dowson and P. J. Sadler, Biguanide Iridium(III) Complexes with Potent Antimicrobial Activity, *J. Med. Chem.*, 2018, **61**, 7330–7344.
14 B. P. R. Aradhyula, M. Kalidasan, K. Gangele, D. K. Deb, S. L. Shepherd, R. M. Phillips, K. M. Poluri and M. R. Kollipara, Synthesis, Structural and Biological Studies of Some Half-Sandwich d6-Metal Complexes with Pyrimidine-Based Ligands, *ChemistrySelect*, 2017, **2**, 2065–2076.
15 A. B. P. Rao, N. R. Palepu, D. K. Deb, A. Uma, T. Chiranjeevi, B. Sarkar, W. Kaminsky and K. M. Rao, Synthesis, structural, DFT studies and antibacterial evaluation of Cp∗ rhodium and Cp∗ iridium complexes using hydrazide based dipyridyl ketone ligand, *Inorganica Chimica Acta*, 2016, **443**, 126–135.

This journal is © The Royal Society of Chemistry 20xx

16 B. F. Hohlfeld, B. Gitter, C. J. Kingsbury, K. J. Flanagan, D. Steen, G. D. Wieland, N. Kulak, M. O. Senge and A. Wiehe, Dipyrrinato-Iridium(III) Complexes for Application in Photodynamic Therapy and Antimicrobial Photodynamic Inactivation, *Chemistry – A European Journal*, 2021, **27**, 6440–6459.

17 L. Shadap, N. Agarwal, V. Chetry, K. M. Poluri, W. Kaminsky and M. R. Kollipara, Arene ruthenium, rhodium and iridium complexes containing benzamide derivative ligands: Study of interesting bonding modes, antibacterial, antioxidant and DNA binding studies, *Journal of Organometallic Chemistry*, 2021, **937**, 121731.

18 N. Baartzes, A. Jordaan, D. F. Warner, J. Combrinck, D. Taylor, K. Chibale and G. S. Smith, Antimicrobial evaluation of neutral and cationic iridium(III) and rhodium(III) aminoquinoline-benzimidazole hybrid complexes, *European Journal of Medicinal Chemistry*, 2020, **206**, 112694.

19 M. Pandrala, F. Li, M. Feterl, Y. Mulyana, J. M. Warner, L. Wallace, F. R. Keene and J. G. Collins, Chlorido-containing ruthenium(ii) and iridium(iii) complexes as antimicrobial agents, *Dalton Trans.*, 2013, **42**, 4686–4694.

20 N. Jain, P. Alam, I. R. Laskar and J. Panwar, 'Aggregation induced phosphorescence' active iridium(iii) complexes for integrated sensing and inhibition of bacterial growth in aqueous solution, *RSC Adv.*, 2015, **5**, 61983–61988.

21 E. Sauvageot, M. Elie, S. Gaillard, R. Daniellou, P. Fechter, I. J. Schalk, V. Gasser, J.-L. Renaud and G. L. A. Mislin, Antipseudomonal activity enhancement of luminescent iridium(iii) dipyridylamine complexes under visible blue light, *Metallomics*, 2017, **9**, 1820–1827.

22 Q.-Y. Yi, W.-Y. Zhang, M. He, F. Du, X.-Z. Wang, Y.-J. Wang, Y.-Y. Gu, L. Bai and Y.-J. Liu, Anticancer and antibacterial activity in vitro evaluation of iridium(III) polypyridyl complexes, *JBIC Journal of Biological Inorganic Chemistry*, 2019, **24**, 151–169.

23 A. Gupta, P. Prasad, S. Gupta and P. K. Sasmal, Simultaneous Ultrasensitive Detection and Elimination of Drug-Resistant Bacteria by Cyclometalated Iridium(III) Complexes, *ACS Appl. Mater. Interfaces*, 2020, **12**, 35967–35976.

24 L. Lu, L.-J. Liu, W. Chao, H.-J. Zhong, M. Wang, X.-P. Chen, J.-J. Lu, R. Li, D.-L. Ma and C.-H. Leung, Identification of an iridium(III) complex with anti-bacterial and anti-cancer activity, *Scientific Reports*, 2015, **5**, 14544.

25 L. Viganor, A. C. M. Galdino, A. P. F. Nunes, K. R. N. Santos, M. H. Branquinha, M. Devereux, A. Kellett, M. McCann and A. L. S. Santos, Anti-Pseudomonas aeruginosa activity of 1,10-phenanthroline-based drugs against both planktonic- and biofilm-growing cells, *Journal of Antimicrobial Chemotherapy*, 2016, **71**, 128–134.

26 M. McCann, A. Kellett, K. Kavanagh, M. Devereux and A. L.S. Santos, Deciphering the Antimicrobial Activity of Phenanthroline Chelators, *Current Medicinal Chemistry*, 2012, **19**, 2703–2714.

27 L. Viganor, O. Howe, P. McCarron, M. McCann and M. Devereux, The Antibacterial Activity of Metal Complexes Containing 1,10-phenanthroline: Potential as Alternative Therapeutics in the Era of Antibiotic Resistance, *Current Topics in Medicinal Chemistry*, 2017, **17**, 1280–1302.

28 V. Novohradsky, G. Vigueras, J. Pracharova, N. Cutillas, C. Janiak, H. Kostrhunova, V. Brabec, J. Ruiz and J. Kasparkova, Molecular superoxide radical photogeneration in cancer cells by dipyridophenazine iridium(iii) complexes, *Inorg. Chem. Front.*, 2019, **6**, 2500–2513.

29 J.-J. Cao, Y. Zheng, X.-W. Wu, C.-P. Tan, M.-H. Chen, N. Wu, L.-N. Ji and Z.-W. Mao, Anticancer Cyclometalated Iridium(III) Complexes with Planar Ligands: Mitochondrial DNA Damage and Metabolism Disturbance, *J. Med. Chem.*, 2019, **62**, 3311–3322.

30 J.-H. Zhao, Y.-X. Hu, H.-Y. Lu, Y.-L. Lü and X. Li, Progress on benzimidazole-based iridium(III) complexes for application in phosphorescent OLEDs, *Organic Electronics*, 2017, **41**, 56–72.

31 F. Monti, A. Baschieri, L. Sambri and N. Armaroli, Excited-State Engineering in Heteroleptic Ionic Iridium(III) Complexes, *Acc. Chem. Res.*, 2021, **54**, 1492–1505.

32 J. P. Cerón-Carrasco, J. Zúñiga and A. Requena, Tuning the Optical Properties of Novel Antitumoral Drugs Based on Cyclometalated Iridium(III) Complexes, *J. Phys. Chem. A*, 2019, **123**, 8644–8649.

33 P. Dreyse, M. Santander-Nelli, D. Zambrano, L. Rosales and L. Sanhueza, Electron-donor substituents on the dppz-based ligands to control luminescence from dark to bright emissive state in Ir(III) complexes, *International Journal of Quantum Chemistry*, 2020, **120**, e26167.

34 J. Weynand, H. Bonnet, F. Loiseau, J.-L. Ravanat, J. Dejeu, E. Defrancq and B. Elias, Targeting G-Rich DNA Structures with Photoreactive Bis-Cyclometallated Iridium(III) Complexes, *Chemistry – A European Journal*, 2019, **25**, 12730–12739.

35 W. Xu, F. Wittich, N. Banks, J. Zink, J. N. Demas and B. A. DeGraff, Quenching of Luminescent Ruthenium(II) Complexes by Water and Polymer-Based Relative Humidity Sensors, *Appl Spectrosc*, 2007, **61**, 1238–1245.

36 G. L. French, Bactericidal agents in the treatment of MRSA infections—the potential role of daptomycin, *Journal of Antimicrobial Chemotherapy*, 2006, **58**, 1107–1117.

37 H. I. Zgurskaya, C. A. López and S. Gnanakaran, Permeability Barrier of Gram-Negative Cell Envelopes and Approaches To Bypass It, *ACS Infect. Dis.*, 2015, **1**, 512–522.

38 Z. V. Feng, I. L. Gunsolus, T. A. Qiu, K. R. Hurley, L. H. Nyberg, H. Frew, K. P. Johnson, A. M. Vartanian, L. M. Jacob, S. E. Lohse, M. D. Torelli, R. J. Hamers, C. J. Murphy and C. L. Haynes, Impacts of gold nanoparticle charge and ligand type on surface binding and toxicity to Gram-negative and Gram-positive bacteria, *Chem. Sci.*, 2015, **6**, 5186–5196.

39 Vaara M, Agents that increase the permeability of the outer membrane, *Microbiological Reviews*, 1992, **56**, 395–411.

40 S. V. Kumar, S. Ø. Scottwell, E. Waugh, C. J. McAdam, L. R. Hanton, H. J. L. Brooks and J. D. Crowley, Antimicrobial Properties of Tris(homoleptic) Ruthenium(II) 2-Pyridyl-1,2,3-triazole "Click" Complexes against Pathogenic Bacteria, Including Methicillin-Resistant Staphylococcus aureus (MRSA), *Inorg. Chem.*, 2016, **55**, 9767–9777.

41 M. A. Kohanski, D. J. Dwyer, B. Hayete, C. A. Lawrence and J. J. Collins, A Common Mechanism of Cellular Death Induced by Bactericidal Antibiotics, *Cell*, 2007, **130**, 797–810.

42 B.-B. Chen, N.-L. Pan, J.-X. Liao, M.-Y. Huang, D.-C. Jiang, J.-J. Wang, H.-J. Qiu, J.-X. Chen, L. Li and J. Sun, Cyclometalated iridium(III) complexes as mitochondria-targeted anticancer and antibacterial agents to induce both autophagy and apoptosis, *Journal of Inorganic Biochemistry*, 2021, **219**, 111450.

43 G. Liao, X. Peng, T. Li, Z. Ye, X. Xiang and C. Fu, The Discovery of an Iridium(III) Dimer Complex as a Potent Antibacterial Agent against Non-Replicating Mycobacterium smegmatis, *Polymers*, 2018, **10**, 297–305.

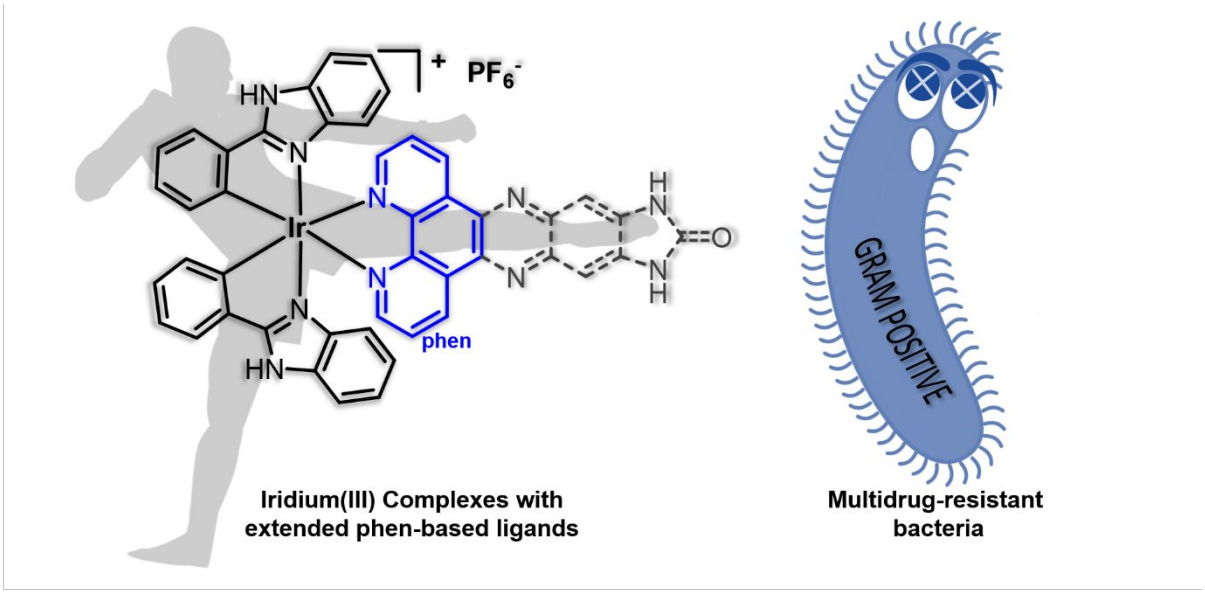
44 E. van Eijk, B. Wittekoek, E. J. Kuijper and W. K. Smits, DNA replication proteins as potential targets for antimicrobials in drug-resistant bacterial pathogens, *Journal of Antimicrobial Chemotherapy*, 2017, **72**, 1275–1284.

45 T. D. M. Pham, Z. M. Ziora and M. A. T. Blaskovich, Quinolone antibiotics, *Med. Chem. Commun.*, 2019, **10**, 1719–1739.

46 C. Griffith, A. S. Dayoub, T. Jaranatne, N. Alatrash, A. Mohamedi, K. Abayan, Z. S. Breitbach, D. W. Armstrong and F. M. MacDonnell, Cellular and cell-free studies of catalytic DNA cleavage by ruthenium polypyridyl complexes containing redox-active intercalating ligands, *Chem. Sci.*, 2017, **8**, 3726–3740.
47 A. T. Dharmaraja, Role of Reactive Oxygen Species (ROS) in Therapeutics and Drug Resistance in Cancer and Bacteria, *J. Med. Chem.*, 2017, **60**, 3221–3240.
48 K. Ulrich and U. Jakob, The role of thiols in antioxidant systems, *Free Radical Biology and Medicine*, 2019, **140**, 14–27.
49 J.-L. Yao, X. Gao, W. Sun, S. Shi and T.-M. Yao, $Ru(bpy)_2$dppz-idzo$]^{2+}$: a colorimetric molecular "light switch" and powerful stabilizer for G-quadruplex DNA, *Dalton Trans.*, 2013, **42**, 5661–5672.
50 Z. Molphy, A. Prisecaru, C. Slator, N. Barron, M. McCann, J. Colleran, D. Chandran, N. Gathergood and A. Kellett, Copper Phenanthrene Oxidative Chemical Nucleases, *Inorg. Chem.*, 2014, **53**, 5392–5404.
51 J. Yellol, S. A. Pérez, G. Yellol, J. Zajac, A. Donaire, G. Vigueras, V. Novohradsky, C. Janiak, V. Brabec and J. Ruiz, Highly potent extranuclear-targeted luminescent iridium(iii) antitumor agents containing benzimidazole-based ligands with a handle for functionalization, *Chem. Commun.*, 2016, **52**, 14165–14168.
52 G. Vigueras, L. Markova, V. Novohradsky, A. Marco, N. Cutillas, H. Kostrhunova, J. Kasparkova, J. Ruiz and V. Brabec, A photoactivated Ir(iii) complex targets cancer stem cells and induces secretion of damage-associated molecular patterns in melanoma cells characteristic of immunogenic cell death, *Inorg. Chem. Front.*, 2021, **8**, 4696–4711.
53 V. Novohradsky, A. Rovira, C. Hally, A. Galindo, G. Vigueras, A. Gandioso, M. Svitelova, R. Bresolí-Obach, H. Kostrhunova, L. Markova, J. Kasparkova, S. Nonell, J. Ruiz, V. Brabec and V. Marchán, Towards Novel Photodynamic Anticancer Agents Generating Superoxide Anion Radicals: A Cyclometalated IrIII Complex Conjugated to a Far-Red Emitting Coumarin, *Angewandte Chemie International Edition*, 2019, **58**, 6311–6315.
54 *Performance standards for antimicrobial susceptibility testing: 17th informational supplement M07-A9*, Clinical and Laboratory Standards Institute., 2012.
55 Carson Christine F., Mee Brian J., and Riley Thomas V., Oil on Staphylococcus aureus Determined by Time-Kill, Lysis, Leakage, and Salt Tolerance Assays and Electron Microscopy, *Antimicrobial Agents and Chemotherapy*, 2002, **46**, 1914–1920.

This journal is © The Royal Society of Chemistry 20xx

Table of contents



The new iridium complexes with phenanthroline-based ligands show great potential as antimicrobials, being even more effective than the broad-spectrum antibiotic norfloxacin in Gram positive bacteria.